JOURNAL OF Materials CHEMISTRY

Structure, epitaxial growth and nucleation of CaO/SrO interfaces using energy minimisation, molecular dynamics and computer graphics

Dean C. Sayle*†

Department of Environmental and Ordnance Systems, Cranfield University, Royal Military College of Science, Shrivenham, Swindon, UK SN6 8LA

Atomistic models of CaO/SrO interfaces have been constructed *via* the sequential deposition of CaO species to SrO surfaces in conjunction with energy minimisation and dynamics. Using this approach the nucleation and growth mechanisms of CaO on the SrO support can be explored. The calculations suggest that the surface of the SrO substrate exacts a critical influence on the structure of the thin film. In particular, surface steps and roughness lead to incoherent films which are difficult to characterise with implications for the surface preparation of support materials. Conversely, the CaO species deposited may also degrade the SrO support: both charged and charge neutral surface vacancies on the SrO surface are created and surface steps are eroded during the deposition process. The results also suggest that the lattice misfit between the two materials is accommodated *via* defects and dislocations within the thin film in addition to considerable structural relaxation of the overlying thin film and the support.

Introduction

The fabrication of many novel materials requires the ability to exercise precise control over the growth of thin films on a host substrate. Indeed, atomic level definition is sometimes required in applications such as supported superconductors, sensors, optical devices and supported catalysts; the presence of even very low concentrations of defects or dislocations may prove deleterious to the particular application or device. Control at the atomic level therefore presents a major challenge to the experimentalist. Simulation studies probing the nucleation and epitaxial growth processes of ultra-thin incommensurate materials would therefore provide a useful complement to the experimental data.

In previous simulation studies[1,2] thin film interfaces were constructed by matching the two (incommensurate) materials using a near coincidence site lattice[3] approach (the interfaces are constructed based on the relative surface geometries of the two materials) and energy minimisation techniques employed to direct the systems to low energy configurations. These studies yielded information on the stability of the interfaces together with insights into how the accommodation of the misfit and interactions across the boundary plane may lead to structural modifications of the thin film. For example, the remarkable catalytic activity observed for V_2O_5 when supported on a TiO_2(annatase) substrate is not evident for either the unsupported V_2O_5 nor the TiO_2 support.[4] Indeed, the catalytic activity of the V_2O_5 thin film is attributed to the structural changes induced in the V_2O_5 by interfacing it with a TiO_2 (annatase) substrate.[2,5] In contrast, for certain applications, such as supported superconductors, structural modifications in the superconducting thin film, resulting from interfacing the superconductor with a support material, may prove deleterious.[6] A solution to this problem has been to deposit a template layer(s) on the substrate material before the superconducting layer is added,[7] the template acting as a kind of buffer for the misfit, accommodating high concentrations of defects, dislocations and induced low crystallinity so damaging to the superconducting properties.

However, such a geometrical approach yields little or no information on the nucleation and growth mechanisms that might direct the material into adopting certain configurations. It is therefore desirable to model the effects of nucleation and growth, and how these factors may influence the structure of the thin film such that a better correlation between theory and experiment may be achieved. Theoretical studies by Kubo *et al.*[8–10] were performed to address these issues. In particular the authors 'grew' the interface by depositing ions, comprising the overlayer, onto the substrate and investigated, using molecular dynamics simulation, the homoepitaxial growth of MgO on MgO(001),[8] and the heteroepitaxial growth of Au on MgO(001)[9] and SrO and BaO on $SrTiO_3$(001).[10] The latter, to predict the appropriate buffer layer for $YBa_2Cu_3O_{7-x}/SrTiO_3$ hetero-junctions. The thin films were created by the sequential deposition of individual molecules, emitted at a random position 15 Å above the substrate with velocities of 900 ms^{-1} to the substrate surface with further molecules emitted at regular time intervals of 1000 time steps. For the MgO/MgO(001) system, two dimensional epitaxial growth was observed at 300 K which included defects. However, increasing the temperature to 1000 K led to films which contained no defects, in accord with experiment. The simulation experiment therefore indicated the temperatures required for defect free growth. For the BaO and SrO on $SrTiO_3$, the SrO monolayer was observed to grow epitaxially and uniformly on the $SrTiO_3$(001), while the monolayer BaO film on $SrTiO_3$(001) was calculated to suffer a high degree of internal stress. Introducing the SrO buffer layer first, *i.e.* BaO/SrO/$SrTiO_3$, resulted in a system with no observable stress. Hence, the authors suggest that BaO/SrO is an appropriate buffer layer for $YBa_2Cu_3O_{7-x}/SrTiO_3$ hetero-junctions. Clearly, these types of calculation can yield useful information on the growth and fabrication of novel supported materials.

A different approach was taken by Shluger *et al.*[11] who investigated the stabilities of small NaCl clusters on an MgO support using energy minimisation techniques. This work was extended by growing the clusters *via* the sequential deposition of NaCl molecules or individual Na and Cl ions.[12] By considering the growth at three different surfaces, a perfect MgO(001) surface, an isolated step on the surface and a defect on the surface, information on how the substrate directs the growth of the overlying material was derived. The study showed that in addition to factors arising from the misfit between the two materials, both surface steps or defects can lead to incoherent

†E-mail: sayle@rmcs.cranfield.ac.uk

thin films and the formation of grain-boundaries which may prove deleterious to the particular application or device.

In this present study the growth of CaO on various SrO surfaces is considered. In addition the combination of dynamics with energy minimisation is employed, the dynamics simulating the migration of ions across the surface that is expected at high temperature. This approach is likely to result in lower energy configurations and consequently higher quality interface models than either a wholly dynamical or energy minimisation approach.

Theoretical methods and potential models

The calculations presented in this study are based on the Born model of the ionic solid in which the ions interact *via* long range Coulombic interactions and short range, parameterised interactions. In addition, the electronic polarisability is introduced *via* the shell model[13] of the ionic solid. The potential parameters for the CaO and SrO were taken from the study of Bush *et al.*[14] and were optimised together with a range of binary metal oxides concurrently. Accordingly, these parameters are not expected to be the best set available for any particular system. However, the advantage of using a consistent set of parameters is that the comparison with alternative interfaces can more reliably be attributable to factors such as the incommensurate nature of the two materials, rather than to any idiosyncrasies arising from deriving optimum potentials for individual materials. Moreover, there is likely to be a degree of mixing of the ions across the interfacial plane. Clearly, the potential parameters for such a study must be readily transferable. For a more detailed discussion on the transferability of these potentials see ref. 14 and references therein.

The simulations, including lattice and surface construction, energy minimisation and dynamics were performed using the MARVIN code.[15] The program considers the crystal as a stack of planes, periodic in two dimensions and subdivided into two regions: a region I where the ions are allowed to move explicitly, and a region II in which the ions are held fixed relative to each other. Region II may, however, relax as a whole allowing the crystal to either expand or contract. The top of region I is the free surface onto which the CaO species are deposited. The energy minimisations are all performed at zero Kelvin and therefore the models derived reflect low temperature structures.

The molecular dynamics scheme employed in MARVIN is a modification of the NVT ensemble, with the proviso that the surface vectors are held fixed, whilst the effective volume of region I is free to fluctuate. This ensemble is termed NAT; a constant Number of particles, surface Area and Temperature. Temperature regulation is achieved *via* direct velocity scaling, which was found to be perfectly suited for well behaved systems. The simulations described here use the velocity-Verlet algorithm[16] although Gear schemes[17,18] are available within MARVIN. The velocity-Verlet algorithm requires less memory than the Gear scheme and thus was favoured for these large scale simulations.

Cluster deposition

The CaO is deposited on one of three surfaces: SrO(001), SrO(510) and SrO(321). The SrO(001) plane can be described as a 'flat' surface presenting five-coordinate strontium and oxygen species at the interface. The SrO(510) surface can be considered as an array of (011) steps on a (001) surface with an inter-step distance of 10.6 Å; the surface comprises mainly five-coordinate species which lie on the terrace together with four-coordinate ions at the step. Finally the SrO(321) surface is designated the 'rough' surface, exhibiting three- and four-coordinate strontium and oxygen species at the surface. The results should therefore reflect the growth of CaO on various SrO surface preparations.

To reduce the computational cost, periodic boundary conditions must be imposed. Clearly, for modeling incommensurate systems this can be a severe approximation as it is difficult to assign any resulting inhomogeneity in the thin film and subsequent strain in the lattice to either the boundary conditions imposed or the incommensurate nature of the materials. Indeed, it is likely to be a combination of both factors. Consequently, the size of the simulation 'box' was constructed to be as large as can be suitably accommodated within the available computational resources to reduce the errors associated with imposing periodic boundary conditions. In particular the simulation 'box' sizes are 659, 672 and 591 Å^2 (*i.e.* 10×10 surface lattices) for the SrO(001), SrO(510) and SrO(321) surfaces respectively.

A small additional program was written to effect the deposition of the CaO on the SrO surface and was used in conjunction with the MARVIN code which performs the minimisation and dynamics simulations. The code introduces Ca^{2+} and O^{2-} at random positions above the SrO surface and moves the species vertically towards the surface until they are within 2.5 Å from the surface or any previously deposited calcium or oxygen species. Dynamics simulation and energy minimisation is then applied to the calcium and oxygen species deposited (the SrO support is held fixed at this stage), to direct them into low energy positions after which additional Ca^{2+},O^{2-} species are added and the process repeated until the required coverage is achieved (about 140% theoretical monolayer coverage for this present study). Further 'runs' can be performed by repeating the whole process using a 'clean' SrO support. After all the runs have been completed, the lowest energy run, based on the energy of the system after all the CaO have been deposited, is then considered further. In particular the simulation was extended to include dynamics and energy minimisation of the SrO surface in addition to the CaO thin film: for every 10 CaO deposition cycles the system was energy minimised, followed by 1000 cycles of dynamics at 1200 K and a final energy minimisation stage which included a shell model description of the CaO and SrO. The structures and energetics of the interfaces were then examined. Fig. 1 illustrates more clearly the method; the dynamics and minimisation procedures applied are presented in Table 1.

Results

The adsorption energy E_{ADS} of the n_{SrO} species forming the interface on the SrO surface is defined, following an approach used previously[11,19] as

$$E_{ADS} = E_{Ca_nO_n/SrO} - E_{SrO} - \left(\frac{n}{2}\right) E_{Ca_2O_2} \quad (1)$$

where $E_{Ca_nO_n/SrO}$ is the total energy of the interface, E_{SrO}, the energy of the substrate and $E_{Ca_2O_2}$, the energy of a Ca_2O_2 molecule. E_{ADS}, which essentially represents the stability of the interface, can usefully be decomposed into three components:

$$E_{ADS} = E_{SP} + E_{INT} + E_C \quad (2)$$

where E_{SP} is the energy associated with the surface perturbation of the support as a result of the overlying CaO, E_{INT}, the interaction energy between the SrO support and the CaO overlayer and E_C the 'cluster' energy of the overlying CaO film, *i.e.*

$$E_C = E_{Ca_nO_n} - \left(\frac{n}{2}\right) E_{Ca_2O_2} \quad (3)$$

where $E_{Ca_nO_n}$ is the energy of the 'isolated' CaO thin film and $E_{Ca_2O_2}$, the energy of a Ca_2O_2 molecule which is calculated as -65 eV using the potential parameters employed in this study.

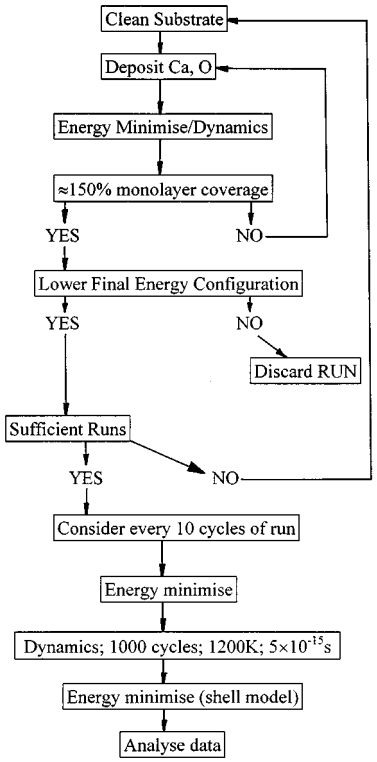

Fig. 1 Flow diagram illustrating the procedure used for depositing the CaO species onto the SrO substrate

Table 1 Dynamics and energy minimisation procedures employed to direct the CaO to low energy configurations on the flat, step and rough surfaces of the SrO substrate

		dynamics		
surface	run	cycles	temperature/K	energy minimisation (every *n* cycles)
flat	1–6	20	800	—
step	1[a]	20	1200	10
	2	200	1000	10
	3	60	1200	—
	4	20	1600	10
rough	1	20	1200	—
	2	20	1200	—
	3	20	1200	—
	4	20	1900	—
	5	5	1900	—
	6	25	600	—
	7[a]	40	1000	10

[a]Depicts lowest energy run.

Fig. 2–5 give E_{SP}, E_{INT}, E_C and E_{ADS}, respectively, as a function of CaO species added for deposition on the flat, step and rough SrO surfaces. In addition, Fig. 6(a)–(c) present the relative contributions made to the adsorption energy by each of the three components, E_{SP}, E_{INT} and E_C as a function of

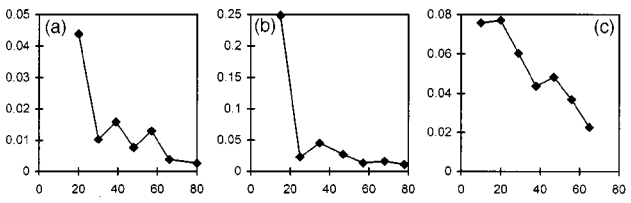

Fig. 2 Calculated surface perturbation energies, E_{SP} (y-axis/J m^{-2}), per molecule of CaO as a function of CaO deposition (x-axis): (a) SrO(001) or flat surface; (b) SrO(510) or step surface and (c) SrO(321) or rough surface

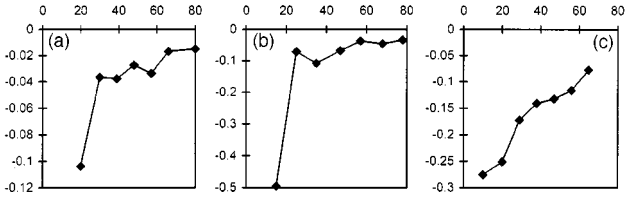

Fig. 3 Calculated interaction energies, E_{INT} (y-axis/J m^{-2}), per molecule of CaO as a function of CaO deposition (x-axis): (a) SrO(001) or flat surface; (b) SrO(510) or step surface and (c) SrO(321) or rough surface

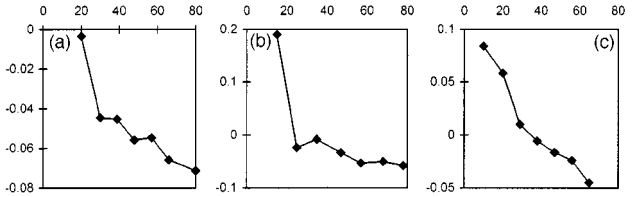

Fig. 4 Calculated cluster energies, E_C (y-axis/J m^{-2}), per molecule of CaO as a function of CaO deposition (x-axis): (a) SrO(001) or flat surface; (b) SrO(510) or step surface and (c) SrO(321) or rough surface

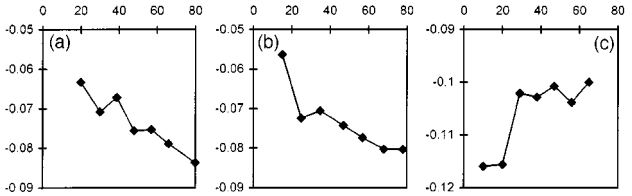

Fig. 5 Calculated adsorption energies, E_{ADS} (y-axis/J m^{-2}), per molecule of CaO as a function of CaO deposition (x-axis): (a) SrO(001) or flat surface; (b) SrO(510) or step surface and (c) SrO(321) or rough surface

CaO deposition. Each of the components comprising the adsorption energy is now considered.

The surface perturbation energies, E_{SP}, [Fig. 2(a)–(c)] give an indication of how the deposition of the CaO species modifies the underlying support material. At low CaO coverage, the perturbation of the support is high and decreases with increasing surface coverage, converging to low but finite values as the surface ions of the support become fully coordinated by the CaO thin film. The results also suggest that the lower the coordination of the surface ions the greater the perturbation. For 15 CaO species deposited on the SrO stepped surface, the perturbation energy is particularly high, almost an order of magnitude higher than for 25 species deposited on the step. Closer inspection of the structure reveals that the step has broken up. In particular, the SrO species comprising the step have migrated to associate with the CaO species deposited. This feature is discussed in more detail later.

The interaction energies, E_{INT}, [Fig. 3(a)–(c)] loosely reflect the adhesion of the thin film with the substrate and are observed to be highest at low CaO deposition and decrease rapidly for the perfect and stepped surfaces. For the rough surface, the decrease in the interaction energy with deposition is almost linear. Indeed, the interaction energy is the major component of the adsorption energy for all deposition levels [Fig. 6(c)].

The 'cluster' energy, E_C, [Fig. 4(a)–(c)] is the difference in energy between the 'isolated' CaO overlayer and $n(Ca_2O_2)$ molecules which comprise this thin film and will be greatest when the CaO adopts a rocksalt type structure. Interfacial interactions between the CaO thin film and SrO support will lead to structural modifications of the CaO leading to a reduction in the value of E_C. The cluster energy therefore

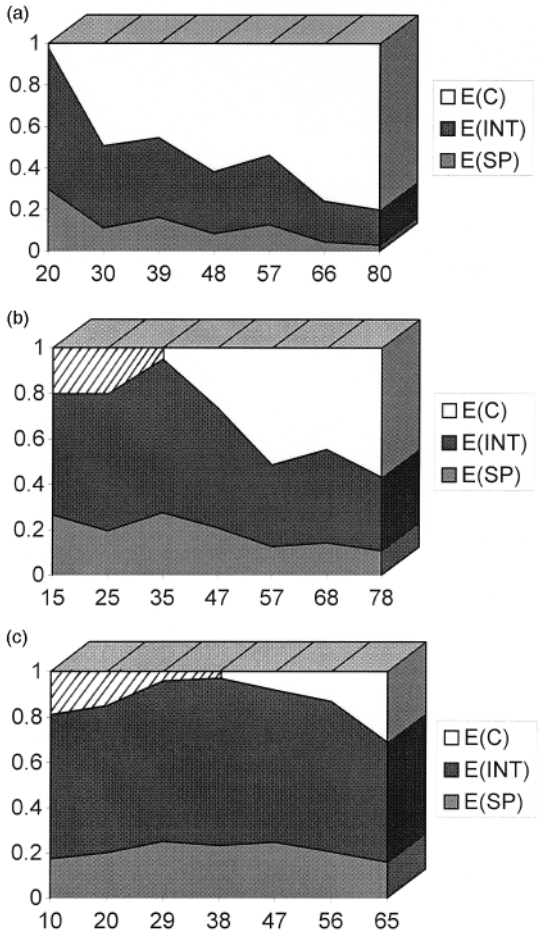

Fig. 6 Relative contributions of E_C, E_{INT} and E_{SP} (y-axis) comprising the adsorption energy E_{ADS} as a function of CaO deposition (x-axis): (a) SrO(001) or flat surface; (b) SrO(510) or step surface and (c) SrO(321) or rough surface. The hatched regions [(b) and (c)] represent negative cluster energies.

provides a measure of how much the support influences the structure of the CaO overlayer, loosely reflecting the coherence of the thin film. Remarkably for the stepped and rough surfaces, the CaO adopts configurations which are less stable than isolated Ca_2O_2 molecules: positive cluster energies are calculated for CaO depositions up to 29 CaO species for the rough surface and 20 for the step. The interactions between the SrO and CaO for these deposition levels outweighing the structural modifications in the CaO required to obtain such interactions, *i.e.* the gain in the interaction energy, E_{INT} exceeds the reduction of E_C: for the step and more particular the rough SrO surface, the interaction energy is the largest component of the adsorption energy [Fig. 6(b) and (c)], while for the perfect surface, the cluster energy [Fig. 6(a)], dominates.

Finally the adsorption energy, E_{ADS}, [Fig. 5(a)–(c)] is the energy released when $(CaO)_2$ molecules are adsorbed on the SrO surface and provides a measure of the interfacial stability. The calculations suggest that the CaO is adsorbed most strongly on the rough surface for all coverages. For the final interface configurations, the adsorption energy for the rough surface is about 25% greater than that calculated for the flat or step surfaces.

The Coulombic, short range and polarisation components of the energy for the flat, step and rough SrO surfaces have also been calculated for the final interface structures. For the surface perturbation and cluster energies the relative proportions of the Coulombic and short range components are essentially equivalent, comprising 88 and 12% of the total energy respectively. However, for the interaction energy the repulsive terms account for a much higher proportion of the total energy. Indeed, for the flat surface, 39% of the interaction energy comprises short range repulsion, indicating like-charged ions are constrained to be in close proximity arising from the incommensurate nature of the system. The driving force for such behaviour is the energy gain resulting from the CaO thin film achieving a reasonably coherent (rocksalt) structure; for the flat surface with 80 CaO species deposited, the cluster energy accounts for 80% of the interfacial stability [Fig. 6(a)].

The calculations also suggest that the polarisation energy contribution to the cluster energy is an order of magnitude higher compared with its contribution to the surface perturbation energy, reflecting the defective nature of the CaO thin films.

Structural considerations [(001) SrO surface]

Various ways of rationalising the structures of the CaO/SrO interfaces have been considered, including radial distribution functions, bond angles and coordination numbers. However, such measures are not wholly effective as the distributions are very broad due to the considerable relaxation and defective nature of these systems. Accordingly, computer graphics has been employed to interpret the structure of these systems. Analysis of the structures can also be problematic owing to the almost infinite number of different configurations that may arise during the deposition process. Consequently, only the salient details and trends that are expected to be universal are presented.

Based on the rocksalt structure of CaO, the theoretical monolayer coverage of the SrO(001) surface (659 $Å^2$) would require the deposition of about 58 CaO species. Therefore each CaO unit represents roughly 1.7% SrO surface coverage.

Fig. 7(a)–(e) show the growth pattern of CaO on the SrO(001) or flat surface after 20, 30, 48 and 80 CaO species have been added to the surface. For 20 CaO species, discrete CaO clusters are clearly visible with the calcium and oxygen species lying about 2.2–2.6 Å directly above their corresponding oxygen and strontium counter-ions of the support. Close inspection of the structure reveals that a single oxygen ion has migrated out of the SrO surface to form part of a CaO cluster, leaving a vacancy on the surface of the support. In addition, an oxygen ion, adjacent to this vacancy, has migrated to an interstitial position midway between two strontium ions. The defect cluster therefore comprises two oxygen vacancies bridged by an oxygen interstitial (Fig. 8). This defective region in the support induces a perturbation in the structure of the overlying CaO cluster which responds by adopting a hexagonal as opposed to cubic symmetry. The positions of the defect cluster and migrated oxygen are indicated by the arrows in Fig. 7(a). This 'defect' structure is only one of many possibilities that are likely to arise during the deposition process. However, in more general terms, the simulation suggests that defects are induced within the support material which may, in turn, influence the structure of the growing overlayer.

After 30 CaO species have been added [Fig. 7(b)], the clusters coalesce and CaO 'chains' are formed, connecting the clusters. One particular chain [at the center of Fig. 7(b)], comprising 8 ions, projects about 6 Å out of the surface plane. The calculations also suggest the CaO does not completely cover the SrO surface with a monatomically flat film, rather bilayers begin to form at about 80% of the theoretical monolayer loading of CaO [Fig. 7(c)].

At 140% loading (80 CaO species), the CaO clearly exhibits the rocksalt structure [Fig. 7(d) and (e)], presenting the (001) surface at the interface. The CaO thin film comprises a bilayer with about 40 CaO species in each layer. In addition, about 25% of the second layer lies above unoccupied regions of the first (interfacial) CaO plane, leaving only 10% of the underlying

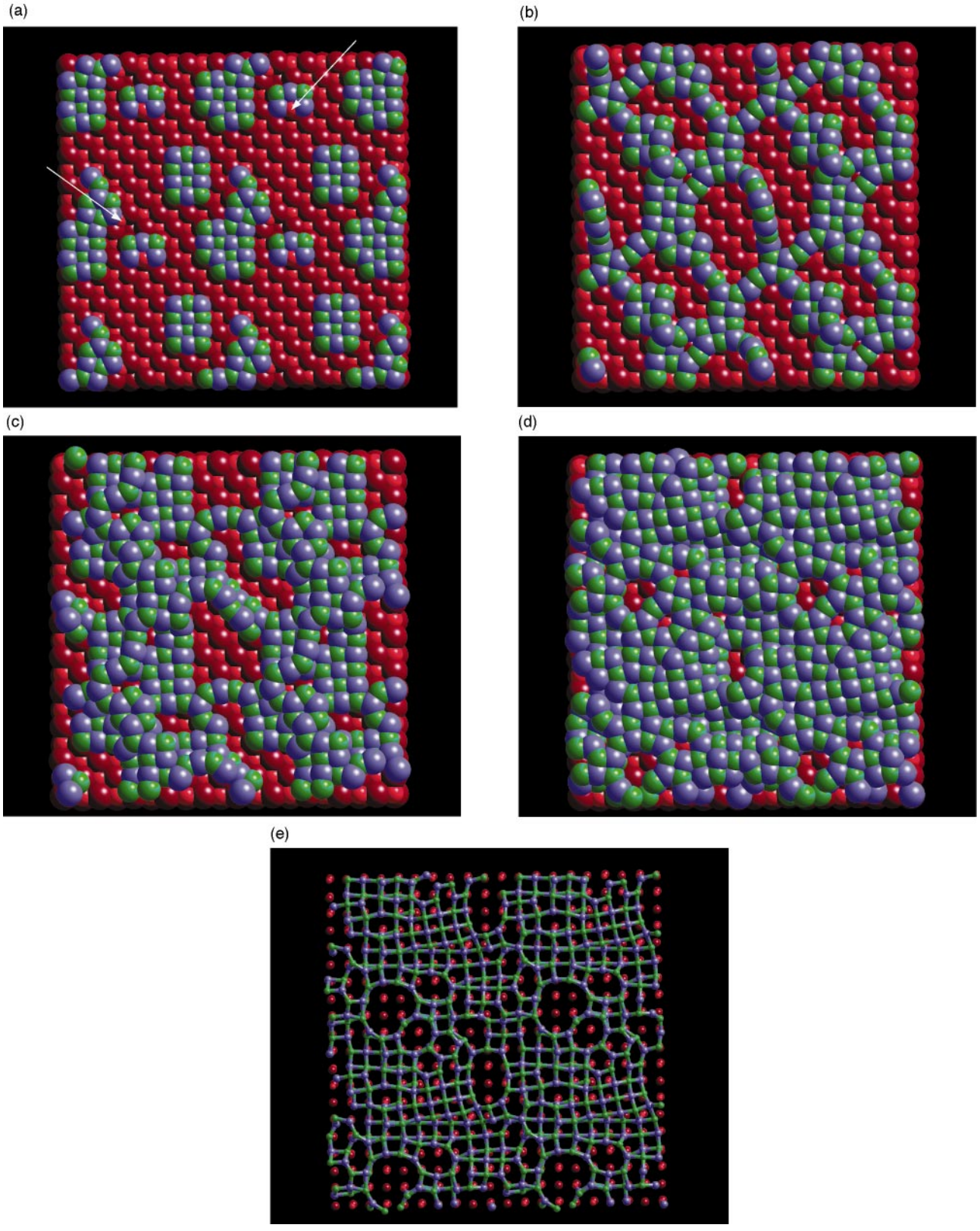

Fig. 7 Diagrammatic representation of the relaxed configurations of CaO species on the SrO(001) or flat surface after the deposition of (a) 20 CaO species; (b) 30 CaO species; (c) 48 CaO species; (d) 80 CaO species and (e) 80 CaO species with ball and stick representation of the CaO thin film. Strontium is coloured dark red, calcium is blue, oxygen (SrO) is light red and oxygen (CaO) is green.

SrO substrate exposed. Fig. 7 also suggests the presence of charged and charge neutral defects. In addition, part of the CaO in the second layer appears to have rotated by about 11°. The driving force to such behaviour is to enable the CaO species to lie directly above their respective counter-ions in the underlying SrO substrate thus maximising the favourable interactions across the boundary plane. Rotations within the film may also be described as dislocations within the CaO structure.

SrO(510) surface or stepped surface

The (510) surface can be described as a stepped surface with a inter-step separation of about 10.6 Å. Fig. 9(a)–(d) present

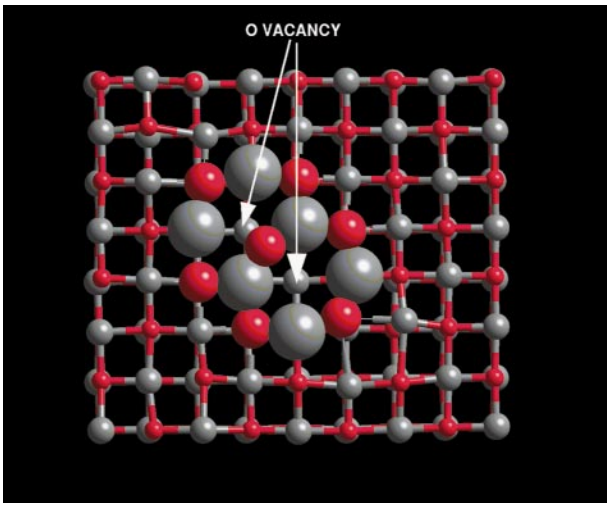

Fig. 8 Diagrammatic representation of the defect cluster comprising two oxygen vacancies bridged by an oxygen interstitial. The CaO species are not shown for reasons of clarity. Oxygen is coloured red and strontium grey.

the configurations of 25, 35, 68 and 78 CaO species deposited onto the stepped surface respectively. Initially, the CaO deposits on the SrO with calcium and oxygen species lying directly above their respective counter-ions and small CaO clusters with the rocksalt type structure are evident [Fig. 9(a)]. However, as the surface coverage increases, the influence of the step induces a considerable structural modification of the CaO away from the rocksalt structure. Indeed, Fig. 9(d) (78 CaO species or 140% theoretical monolayer coverage) suggests that the CaO appears to adopt hexagonal symmetry. For most simple rocksalt structured oxides, the distance between steps is likely to be high, $\gg$11 Å, and therefore the surface would comprise predominantly the plateau region of the stepped surface, *i.e.* SrO(001).

The results thus far suggest that the support influences the structure of the thin film. However, the CaO deposited may also perturb the support: for the perfect surface oxygen vacancies were created. For the step surface, the effect on the support is more profound and is discussed in the following section.

Fig. 10(a)–(c) show three representations of the SrO stepped surface with 15 CaO species deposited on the surface. Fig. 10(a) shows the edge of the first step (vertical arrow) which includes an adjacent Sr,O vacancy lying along the step edge (top arrow). These ions have migrated out of the step to form part of a CaO cluster on the SrO surface. Fig. 10(b) highlights adjacent

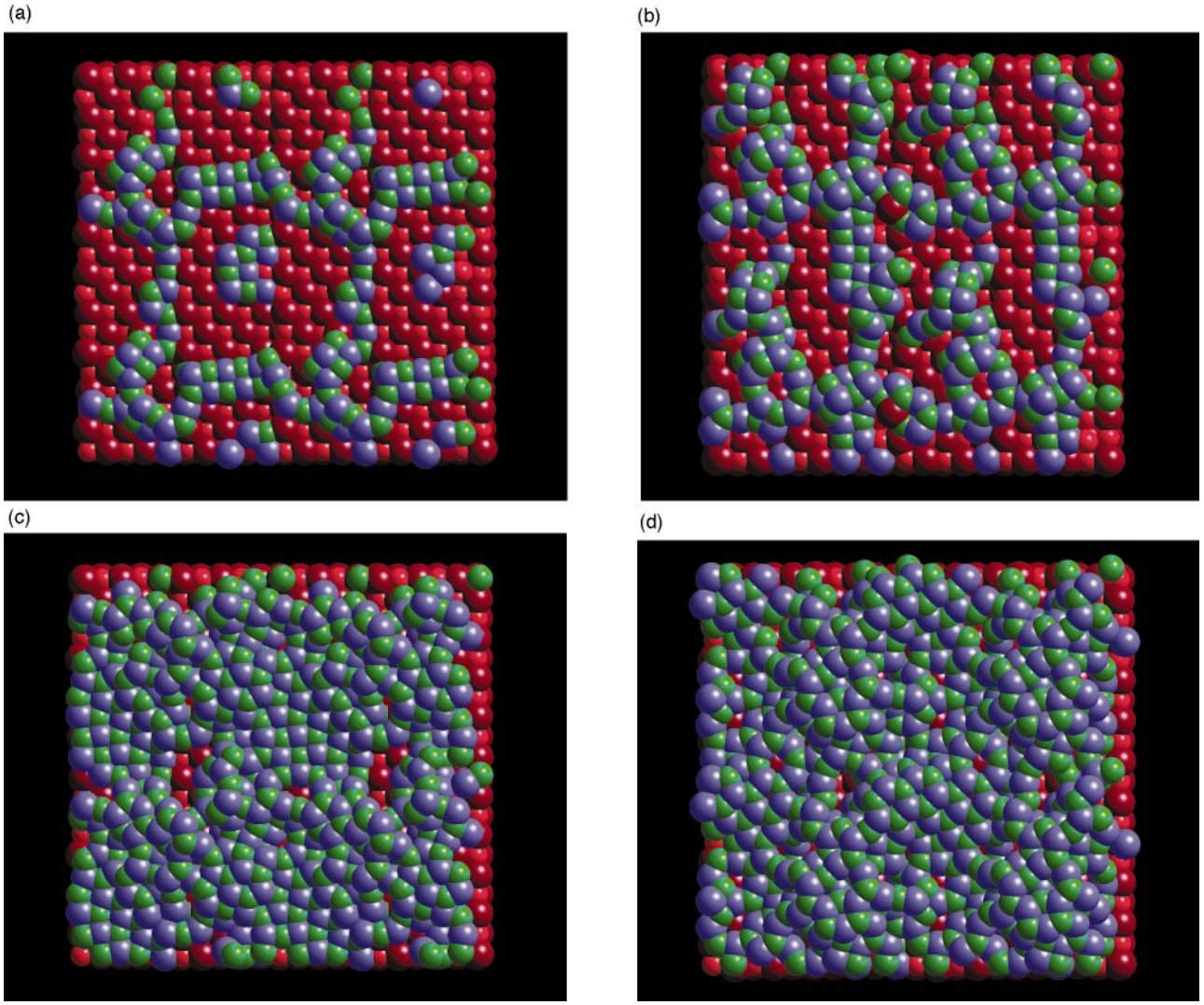

Fig. 9 Diagrammatic representation of the relaxed configurations of CaO species on the SrO(510) or step surface after the deposition of (a) 25 CaO species; (b) 35 CaO species; (c) 68 CaO species and (d) 78 CaO species. Strontium is coloured dark red, calcium is blue, oxygen (SrO) is light red and oxygen (CaO) is green.

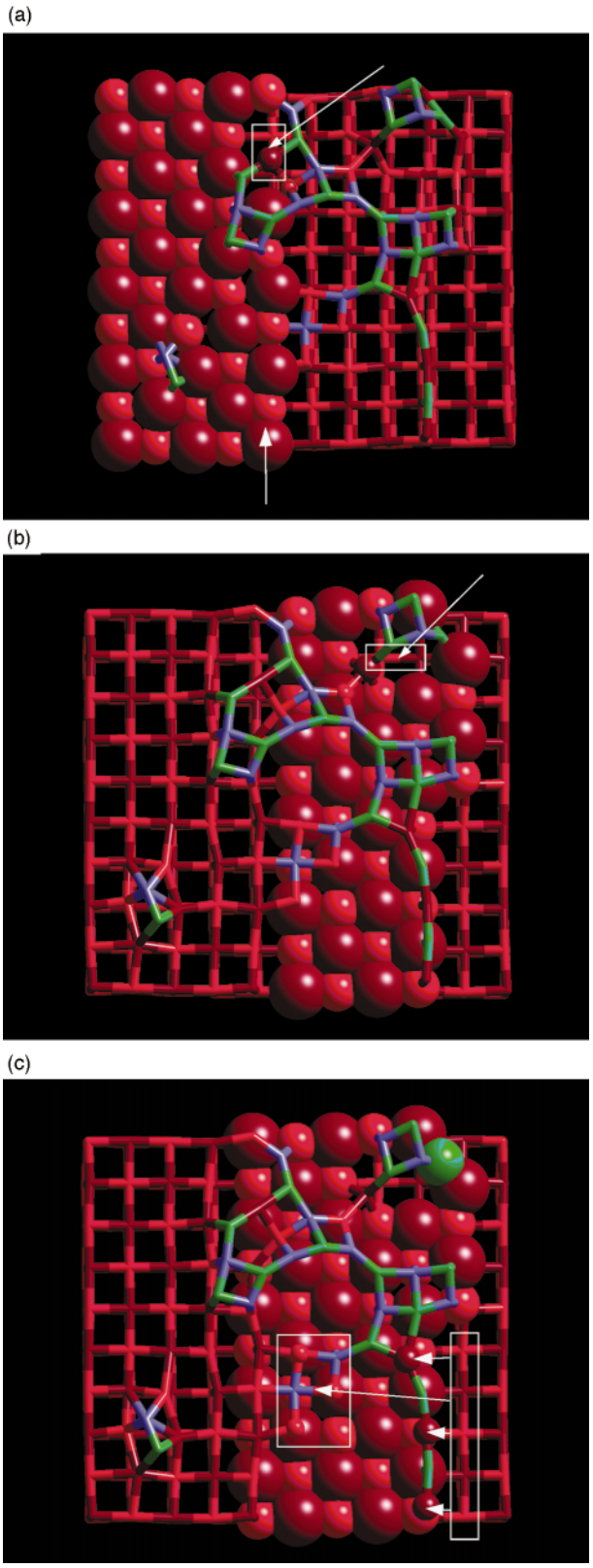

Fig. 10 Diagrammatic representation of the relaxed configurations of 15 CaO species on the SrO(510) or step surface illustrating: (a) SrO vacancy on the step; (b) SrO vacancy on the plateau region of the step and (c) migration of three SrO species from the step. Strontium is coloured dark red, calcium is blue, oxygen (SrO) is light red and oxygen (CaO) is green.

Sr,O vacancies which have migrated from the plateau region of the stepped surface to associate with the CaO species deposited. In addition Fig. 10(c) reveals three Sr,O species which have migrated from the edge of the second step, as illustrated by the arrows. The results therefore suggest that the CaO species deposited, have the potential to 'erode' the surface and step regions of the SrO support, creating vacancies and areas of reduced coordinative saturation at the step. Moreover, such regions are expected to provide additional nucleation centers.

SrO(321) surface or rough surface

The relaxed structures of 20, 29, 56 and 65 CaO species adsorbed on the SrO(321) surface are presented in Fig. 11(a)–(d). The initial growth [Fig. 11(a)] suggests that the CaO begins to reproduce the (321) surface structure, which acts as template in directing the growth of the thin film. However, such growth cannot be sustained as the incommensurate nature of the system would result in prohibitively large strains within the CaO clusters. Accordingly, after the deposition of 65 CaO species, the thin film structure does not conform to the surface structure presented by the host substrate and appears almost amorphous.

Conclusions

In this study thin CaO films on an SrO support have been constructed *via* the sequential deposition of single calcium and oxygen ions to the SrO surface including dynamics and energy minimisation to direct the species to low energy configurations. Using this approach, an understanding of the epitaxial growth and nucleation processes can be explored. At low coverage, CaO clusters which initially reproduce the structure of the underlying support are observed, the support acting as a kind of template in directing the growth of the adsorbed species. On further CaO deposition, these clusters coalesce to form chain-like structures. Complete monolayer coverage of the SrO support by CaO does not occur, rather the CaO grows to form a bilayer before the monolayer completely covers the surface. The final interface structures exhibit considerable structural relaxation and comprise defects, both charged and charge neutral, together with dislocations in the CaO overlayer.

The SrO surface exposed also plays a significant role in determining the growth of the CaO. The flat SrO(001) surface yields the most coherent films, consistent with the rocksalt structure, while SrO surfaces, exposing a high concentration of steps or surface roughness, perturb the CaO growth leading to poorer quality films with implications for the surface preparation of the substrate material. In addition, the deposition of CaO species also influences the structure of the SrO support: surface steps are eroded and vacancies created on the surface of the support creating additional nucleation centers for the growth of the CaO overlayer.

The most stable interface identified was the CaO/SrO(321) or 'rough' surface, being 25% more stable than that calculated for the CaO/SrO(001) system. However this value gives no indication of the thin film quality. Indeed, for this system, the CaO structure appeared amorphous.

Experimentally, the misfit between two interfaced materials has been shown be accommodated by the presence of defects and/or dislocations both in the thin film overlayer[20,21] and the support[22] in accord with our interface models. Such defects, as suggested previously, may prove deleterious to the potential application of the supported material.[7] Simulation techniques may therefore provide an inexpensive way to correlate the lattice misfit and substrate quality (*i.e.* surface preparation) with the structure and coherence of the resulting thin film and, in addition, may be employed to predict an effective buffer layer.

D.C.S would like to thank Roger Cox for help in generating the computer graphics and David Gay and Ben Slater for help with the MARVIN code.

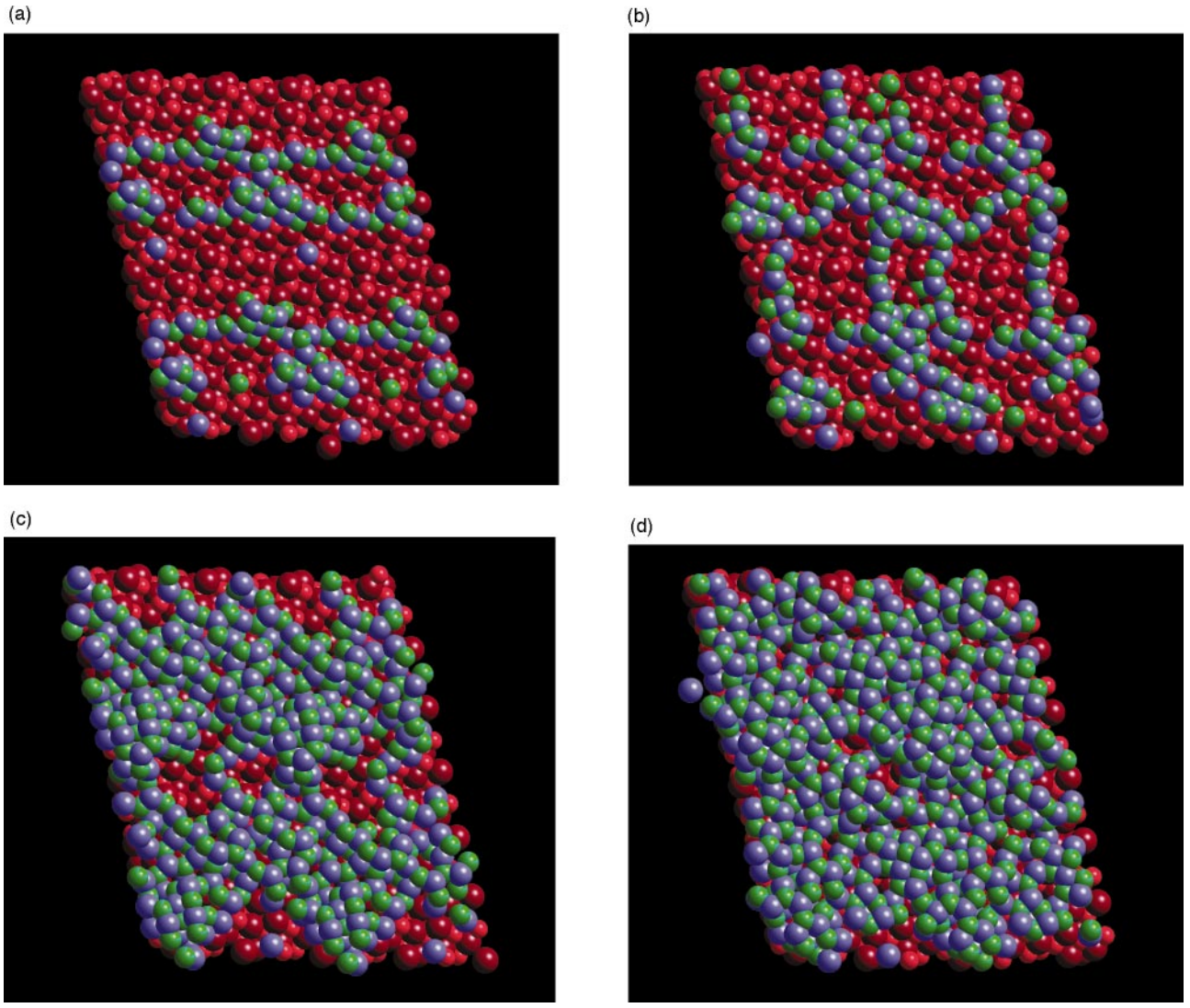

Fig. 11 Diagrammatic representation of the relaxed configurations of CaO species on the SrO(321) or rough surface after the deposition of (a) 20 CaO species; (b) 29 CaO species; (c) 56 CaO species and (d) 65 CaO species. Strontium is coloured dark red, calcium is blue, oxygen (SrO) is light red and oxygen (CaO) is green.

References

1 T. X. T. Sayle, C. R. A. Catlow, D. C. Sayle, S. C. Parker and J. H. Harding, *Philos. Mag. A*, 1993, **68,** 565.
2 D. C. Sayle, C. R. A. Catlow, M.-A. Perrin and P. Nortier, *J. Phys. Chem*., 1996, **100,** 8940.
3 H. Grimmer, W. Bollmann and D. H. Warrington, *Acta Crystallogr*., 1974, **30,** 197.
4 G. C. Bond, S. Flamerz and R. Shukri, *Faraday Discuss*., *Chem. Soc*., 1989, **87**, 65.
5 G. Centi, E. Giamello, D. Pinelli and F. Trifiro, *J. Catal*., 1991, **130**, 220.
6 D. Dimos, P. Chaudhari and J. Mannhart, *Phys. Rev. B*, 1990, **41**, 4038.
7 E. Olsson, A. Gupta, M. D. Thouless, A. Segmuller and D. R. Clarke, *Appl. Phys. Lett*., 1991, **58,** 1682.
8 M. Kubo, Y. Oumi, R. Miura, A. Fahmi, A. Stirling, A. Miyamoto, M. Kawasaki, M. Yoshimoto and H. Koinuma, *J. Chem. Phys*., 1997, **107**, 4416.
9 M. Kubo, R. Miura, R. Yamauchi, M. Katagiri, R. Vetrivel, E. Broclawik and A. Miyamoto, *Jpn. J. Appl. Phys*., 1995, **34**, 6873.
10 M. Kubo, Y. Oumi, R. Miura, A. Stirling, A. Miyamoto, M. Kawasaki, M. Yoshimoto and H. Koinuma, *Phys. Rev. B*, 1997, **56**, 13535.
11 A. L. Shluger, A. L. Rohl and D. H. Gay, *Phys. Rev. B*, 1995, **51,** 13 631; A. L. Shluger, A. L. Rohl and D. H. Gay, *J. Vac. Sci. Technol. B*, 1995, **13,** 1190.
12 D. C. Sayle, C. R. A. Catlow and M.-A. Perrin, *Phys. Rev. B*, 1997, **56**, 15952.
13 B. G. Dick and A. W. Overhauser, *Phys. Rev*., 1958, **112,** 90.
14 T. S. Bush, C. R. A. Catlow and P. D. Battle, *J. Mater. Chem*., 1995, **5**, 1269.
15 D. H. Gay and A. L. Rohl, *J. Chem. Soc*., *Faraday Trans*., 1995, **91**, 925.
16 W. C. Swope, H. C. Anderson, P. H. Berens and K. R. Wilson, *J. Chem. Phys*., 1982, **76**, 637.
17 C. W. Gear, *The numerical integration of ordinary differential equations of various orders*, Report ANL 7126, Argonne National Laboratory, 1966.
18 C. W. Gear, *Numerical initial value problems in ordinary differential equations*, Prentice-Hall, Englewood Cliffs, NJ, 1971.
19 D. C. Sayle, PhD Thesis, University of Bath, 1992.
20 O. Eibl, H. E. Hoenig, J.-M. Triscone, O. Fischer, L. Antognazza and O. Brunner, *Physica C*, 1990, **172**, 373.
21 Y. Fujiwara, S. Hirata, M. Iyori and T. Kobayashi, *Solid State Commun*., 1990, **74**, 641.
22 J. Narayan, S. Sharan, R. K. Singh and K. Jagannadham, *Mater. Sci. Eng. B*, 1989, **2**, 333.

Paper 8/03035I; *Received* 23*rd April*, 1998